Acta Geodyn. Geomater., Vol. 14, No. 3 (187), 323–332, 2017
DOI: 10.13168/AGG.2017.0015
journal homepage: https://www.irsm.cas.cz/acta

ORIGINAL PAPER

COMPREHENSIVE ASSESSMENT OF POSITIONING AND ZENITH TOTAL DELAY RETRIEVAL USING GPS+GLONASS PRECISE POINT POSITIONING

Feng ZHOU [1, 2, 4], Shengfeng GU [3, 4], Wen CHEN [1, 2] * and Danan DONG [1, 2]

[1] *Engineering Center of SHMEC for Space Information and GNSS, East China Normal University, No. 500 Dongchuan Road, Shanghai 200241, China*
[2] *Shanghai Key Laboratory of Multidimensional Information Processing, East China Normal University, No. 500 Dongchuan Road, Shanghai 200241, China*
[3] *GNSS Research Center, Wuhan University, Wuhan 430079, China*
[4] *German Research Centre for Geosciences GFZ, Telegrafenberg, Potsdam 14473, Germany*

**Corresponding author's e-mail:* wchen@sist.ecnu.edu.cn

ARTICLE INFO

Article history:
Received 3 March 2017
Accepted 16 May 2017
Available online 2 June 2017

Keywords:
GPS
GLONASS
Precise point positioning (PPP)
Zenith total delay (ZTD)
Antenna/radome-dependent biases

ABSTRACT

Since October 2011, the Russian GLObal NAvigation Satellite System (GLONASS) has been revitalized and is now fully operational with 24 satellites in orbit. It is critical to assess the benefits and problems of using GLONASS observations (i.e. GLONASS-only or combined Global Positioning System (GPS) and GLONASS) for precise positioning and zenith total delay (ZTD) retrieval on a global scale using precise point positioning (PPP) technique. In this contribution, extensive evaluations are conducted with Global Navigation Satellite System (GNSS) data sets collected from 251 globally distributed stations of the International GNSS Service (IGS) network in July 2016. The stations are divided into 30 groups by antenna/radome types to investigate whether there are antenna/radome-dependent biases in position and ZTD derived from GLONASS-only PPP. The positioning results do not show obvious antenna/radome-dependent biases except the stations with JAV_RINGANT_G3T/NONE. For these stations, the averaged biases in horizontal component, especially in the north component, can achieve as high as –9.0 mm. The standard deviation (STD) and root mean square (RMS) are used as indicators of positioning repeatability and accuracy, respectively. The averaged horizontal STD and RMS of GLONASS-only PPP are comparable to GPS-only PPP, while in vertical component, those for GLONASS-only PPP are larger. Furthermore, the STD and RMS of GPS+GLONASS combined PPP solutions are the smallest in horizontal and vertical components, indicating that adding GLONASS observations can achieve better positioning performance than GPS-only PPP. With the IGS final ZTD as reference, we find that ZTD biases and accuracy of GLONASS-only are latitude- and antenna/radome-independent. The ZTD accuracy of GLONASS-only PPP is slightly worse than that of GPS-only PPP. Compared with GPS-only PPP, the ZTD accuracy is only improved by 1.3% from 7.8 to 7.7 mm by adding GLONASS observations.

1. INTRODUCTION

Over the past decades, the Global Positioning System (GPS), known as the first Global Navigation Satellite System (GNSS), has emerged as a powerful tool not only in scientific applications, such as geodesy, remote sensing of atmosphere and ionosphere, but also in engineering services, i.e. surveying, navigation, and timing (Bock and Melgar 2016). As the second global navigation satellite system, Russia's GLObal NAvigation Satellite System (GLONASS) was recovering gradually and there were 13 satellites in orbit in 2007 (Alcay et al., 2012). Since then, great efforts have been focused on the comparison between GPS-only and GPS+GLONASS combined solutions (Zinoviev, 2005; Bruyninx, 2007; Cai and Gao, 2007; Defraigne and Baire, 2011). Among which, Bruyninx (2007) presented a comparative analysis of GPS-only and combined GPS+GLONASS differential positioning in a regional permanent GNSS network. The results suggested that, compared with GPS-only solutions, no obvious improvement in precision could be achieved by combined solution. While regarding the precise point positioning (PPP, Zumberge et al., 1997), Cai and Gao (2007) argued that improvement in terms of both positioning convergence and accuracy is expected, depending on the geometry improvement benefit from additional GLONASS observations of 12 active satellites.

Obviously, due to its inadequate number of satellites for globally independent positioning, GLONASS was only regarded as an auxiliary tool for GPS to improve positioning convergence and accuracy in the above studies. While, GLONASS has been revitalized since October 2011 and is now fully operational with 24 satellites in orbit (https://www.glonass-iac.ru/en/GLONASS/).

Cite this article as: Zhou F, Gu S, Chen W, Dong D: Comprehensive assessment of positioning and zenith delay retrieval using GPS+GLONASS precise point positioning.Acta Geodyn. Geomater., 14, No. 3 (187), 323–332, 2017.
DOI: 10.13168/AGG.2017.0015

Moreover, the number of globally distributed stations with GLONASS tracking capability is increasing (See Figure 2 in Fritsche et al. (2014)). Thus, increasing studies started to explore the performance of GLONASS-only precise positioning (Cai and Gao, 2013; Anquela et al., 2013; Lou et al., 2015). The results of Cai and Gao (2013) based on 15 high-latitude International GNSS Service (IGS) stations indicated that the GLONASS-only PPP can reach an comparable accuracy to GPS-only PPP. Lou et al. (2015) indicated that GLONASS-only PPP performance showed obvious regional characteristics relating to the satellite geometry.

Besides the applications in positioning, GNSS has also been demonstrated as an efficient tool in atmosphere studies, and the first attempt in GLONASS troposphere modeling can be found in the work of Dousa (2010). Based on a European network of 38 stations, Dousa (2010) indicated that the root mean square (RMS) of zenith total delay (ZTD) derived from GLONASS is 1–3 mm larger than that of GPS. The problem of 1.5 mm ZTD average biases was related to the inconsistent GLONASS satellite antenna phase center offsets (PCOs) and variations (PCVs) in igs05.atx models (see Dilssner et al., 2009). With the model updated (from igs05.atx to igs08.atx), Dousa and Vaclavovic (2016) found that the ZTD biases between GPS and GLONASS did not exist any longer. More recently, Lu et al. (2016) analyzed the ZTD derived from GPS-, GLONASS-only, and the combined GPS+GLONASS solutions in a simulated real-time mode and suggested that the ZTD estimates derived from GPS-, GLONASS-only, and the combined GPS+GLONASS solutions agree well with each other.

Along with the successful deployment and application of GLONASS, some data-processing related topics are revealed and explored further. As pointed out by Zheng et al. (2012) from the results with two independent networks using the igs08.atx model, the coordinates derived from GLONASS solutions showed some antenna/radome-dependent systematic biases, varying from several mm to 1 cm for stations with different antenna/radome types. This is further confirmed by Schmid et al. (2016), and their study suggested that the GLONASS positioning biases in vertical with the igs08.atx model were most likely antenna related, i.e., for most stations with Trimble antennas, the biases were negative, while for stations with Leica or Topcon antennas, the biases were positive. In addition, it is found that the initial inconsistency between GPS- and GLONASS-only ZTD solutions disappeared when the igs08.atx model was adopted (Schmid et al., 2016).

The previous studies are mainly on combined GPS+GLONASS differential positioning in a regional network. PPP technique is widely exploited in GNSS precise positioning and meteorology due to its efficiency and flexibility in analyzing GNSS networks with a large number of stations (Baire et al., 2014; Li et al., 2014; He et al., 2016; Liu et al., 2016). It is critical to assess the benefits and problems of using GLONASS observations (i.e. GLONASS-only or combined GPS+GLONASS) for precise positioning and ZTD retrieval on a global scale using PPP technique. In this work, we compare the accuracy of the position estimates of GLONASS-only PPP from using GPS- and GLONASS-specific receiver antenna PCV corrections, respectively. By dividing the selected stations into 30 groups by antenna/radome types, we further assess the positioning biases, repeatability, and accuracy derived from GPS-, GLONASS-only, and GPS+GLONASS PPP solutions. The aim is to investigate antenna/radome-dependent biases in position. Furthermore, we evaluate the ZTD results.

2. GPS+GLONASS IONOSPHERE-FREE OBSERVATION MODEL

Ionosphere-free combined observables are normally utilized to remove the first-order ionospheric delay. The undifferenced GNSS ionosphere-free observations are generally expressed as

$$P^s_{r,IF} = \rho^s_r + dt_r - dt^s + T^s_r + \varepsilon^s_{r,IF} \tag{1}$$

$$L^s_{r,IF} = \rho^s_r + dt_r - dt^s + T^s_r + N^s_{r,IF} + \xi^s_{r,IF} \tag{2}$$

where indices s and r refer to the satellite and receiver, respectively; ρ^s_r denotes the geometric distance between the satellite and receiver; dt_r and dt^s are the clock offsets of the receiver and satellite; T^s_r is the slant tropospheric delay; $N^s_{r,IF}$ is the ionosphere-free phase ambiguity; $\varepsilon^s_{r,IF}$ and $\xi^s_{r,IF}$ are the sum of measurement noise and multipath error for the ionosphere-free pseudorange and carrier phase observations. Note that all the variables in Eqs. (1) and (2) are expressed in meters.

Considering homogeneity and inhomogeneity of the troposphere, the slant tropospheric delay T^s_r is modeled by the sum of hydrostatic, wet, and gradient delay (Chen and Herring, 1997) as follows

$$\begin{aligned} T^s_r = {} & mf_h(e)\cdot Z_h + mf_w(e)\cdot Z_w + \\ & + mf_g(e)\cdot[G_{ns}\cdot\cos(a) + G_{ew}\cdot\sin(a)] \end{aligned} \tag{3}$$

where a, and e is the azimuth and elevation angle of the satellite, respectively. Z_h denotes zenith hydrostatic delay, which can be modeled accurately using empirical models such as Saastamoinen (Saastamoinen, 1973); $mf_h(e)$ and $mf_w(e)$ are the hydrostatic and wet mapping functions that can be retrieved with Global Mapping Function (GMF, Boehm et al., 2006); $mf_g(e)$ is the gradient mapping function (Chen and Herring, 1997). In the GNSS based troposphere modeling, the zenith wet delay Z_w

Table 1 The types of antenna/radome of the selected stations.

Group #	Antenna	Radome	Number of stations	Group #	Antenna	Radome	Number of stations
1	TRM55971.00	NONE	8	16	TPSCR.G5	TPSH	3
2	TRM57971.00	NONE	22	17	TPSCR3_GGD	CONE	4
3	TRM9800.00	NONE	30	18	JAVRINGANT_DM	NONE	7
4	TRM9800.00	SCIS	20	19	JAVRINGANT_DM	SCIS	7
5	LEIAR10	NONE	4	20	JAVRINGANT_DM	JVDM	2
6	LEIAX1202 GG	NONE	2	21	JAV_RINGANT_G3T	NONE	17
7	LEIAT504 GG	NONE	7	22	SEPCHOKE_MC	NONE	5
8	LEIAT504 GG	LEIS	7	23	NOV702GG	NONE	4
9	LEIAR25.R3	NONE	3	24	NOV750.R4	NOVS	2
10	LEIAR25.R3	LEIT	17	25	AOAD/M_T	NONE	13
11	LEIAR25.R4	NONE	7	26	ASH701945C_M	NONE	5
12	LEIAR25.R4	LEIT	21	27	ASH701945D_M	SNOW	2
13	TPSCR.G3	NONE	9	28	ASH701945E_M	NONE	8
14	TPSCR.G3	SCIS	7	29	ASH701945G_M	NONE	2
15	TPSCR.G3	TPSH	3	30	JPSREGANT_SD_E	NONE	3

and gradient vector $\boldsymbol{G} = \begin{pmatrix} G_{ns} & G_{ew} \end{pmatrix}^T$ with north-south and east-west components, are usually estimated as unknowns along with other parameters in PPP processing.

Substituting Eq. (3) into Eqs. (1) and (2), and applying the IGS precise satellite orbit and clock products, the linearized observation model within the combined GPS+GLONASS context can be reformed as

$$\begin{cases} p_{r,IF}^G = \boldsymbol{u}_r^G \cdot \boldsymbol{x} + dt_r + mf_w(e) \cdot Z_w + mf_g(e) \cdot \cos(a) \cdot G_{ns} \\ \quad + mf_g(e) \cdot \sin(a) \cdot G_{ew} + \varepsilon_{r,IF}^G \\ p_{r,IF}^R = \boldsymbol{u}_r^R \cdot \boldsymbol{x} + dt_r + IFB_{R_k,G} + mf_w(e) \cdot Z_w + mf_g(e) \cdot \cos(a) \cdot G_{ns} \\ \quad + mf_g(e) \cdot \sin(a) \cdot G_{ew} + \varepsilon_{r,IF}^R \end{cases} \tag{4}$$

$$\begin{cases} l_{r,IF}^G = \boldsymbol{u}_r^G \cdot \boldsymbol{x} + dt_r + mf_w(e) \cdot Z_w + mf_g(e) \cdot \cos(a) \cdot G_{ns} \\ \quad + mf_g(e) \cdot \sin(a) \cdot G_{ew} + N_{r,IF}^G + \xi_{r,IF}^G \\ l_{r,IF}^R = \boldsymbol{u}_r^R \cdot \boldsymbol{x} + dt_r + mf_w(e) \cdot Z_w + mf_g(e) \cdot \cos(a) \cdot G_{ns} \\ \quad + mf_g(e) \cdot \sin(a) \cdot G_{ew} + N_{r,IF}^R + \xi_{r,IF}^R \end{cases} \tag{5}$$

where the indices G and R refer to GPS and GLONASS satellite systems, respectively; $p_{r,IF}^s$ and $l_{r,IF}^s$ denote observed minus computed (OMC) values of pseudorange and carrier phase observables; $\boldsymbol{u}_r^s$ is the unit vector of the component from the receiver to the satellite; $\boldsymbol{x}$ is the vector of the receiver position increments relative to a priori position; R_k denotes GLONASS satellite with factor k that used for the computation of signal frequency. It is noted that the $IFB_{R_k,G}$ parameter for each station and GLONASS satellite pair in this study is actually the combination of original inter-system bias (ISB) of GPS and GLONASS as well as inter-frequency code bias of GLONASS.

Based on the above discussion, the estimates vector $\boldsymbol{S}$ is expressed as

$$\boldsymbol{S} = [\boldsymbol{x}, dt_r, IFB_{R_k,G}, Z_w, G_{ns}, G_{ew}, \boldsymbol{N}_{r,IF}]^T \tag{6}$$

3. EXPERIMENTAL RESULTS AND ANALYSIS

3.1. DATA AND PROCESSING STRATEGY

To demonstrate how the GLONASS contributes to PPP estimation of coordinates and tropospheric parameters with respect to the receiver antenna PCV effects, comprehensive numerical analyses are conducted with observations collected from 251 globally distributed stations of IGS network during the period of DOY (Day of Year) 183-213, 2016. Figure 1 shows the geographical distribution of the selected stations with GPS and GLONASS tracking capability. Generally, those stations are denoted in green and purple, respectively, depending to the availability of GLONASS-specific antenna phase center corrections. While regarding the antenna/radome involved, the stations are further divided into 30 groups as shown in Table 1.

The Positioning And Navigation Data Analyst (PANDA) software (Liu and Ge, 2003; Gu et al., 2015) is used for experiment demonstration. Three strategies, i.e. GPS-, GLONASS-only, and combined GPS+GLONASS are compared in the data processing. GPS and GLONASS precise orbit and clock products with an interval of 15 min and 30s, respectively, provided by ESA (European Space Agency) are fixed in all these solutions. In addition, the float phase ambiguities are estimated as constant for each continuous satellite arc. The zenith wet delays are estimated as a continuous piecewise linear function with 2 h parameter spacing. The troposphere gradients in north-south and east-west direction have a parameter spacing of 24 h. The elevation-dependent weighting for the observations with elevation angle below 30° is applied, and the weighting ratio of GPS

and GLONASS is assumed to be 1:1 (Lou et al., 2015). Regarding the results evaluation, the positioning performance is assessed with respect to either the coordinates from IGS weekly SINEX (Solution INdependent EXchange format) files, or the averaged values from 7 consecutive daily PPP solutions with the PANDA software in static mode. While, the ZTD estimates are analyzed with respect to the IGS meteorology product.

3.2. PCVS EFFECT ON GLONASS POSITIONING

Since not all the receiver antennas have the GLONASS-specific PCV corrections. It is worth to identify the effect of mis-matching antenna model on GLONASS high-precision data processing before the performance evaluation. This was conducted by the comparison between GLONASS-only PPP with GPS PCVs and without PCVs corrections for the 33 stations (green triangles in Figure 1) that with only GPS-specific antenna/radome PCVs (Group 25-30 in Table 1). Furthermore, concerning the 218 stations that both have GPS- and GLONASS-specific PCVs, GLONASS-only PPP was carried out by using igs08_1918.atx model with GPS- and GLONASS-specific PCV corrections, respectively. It is noted that in all the experiments, the GPS PCOs are applied at ground antennas since they are identical for GPS and GLONASS regardless the antennas equipped as implied by igs08.atx.

Concerning those 33 stations without GLONASS-specific antenna/radome PCOs and PCVs, GPS-specific PCVs are used for the validation. The positioning accuracy and the difference of accuracy are indicated in Figure 2. Compared with no PCV corrections, the averaged vertical RMS of GLONASS-only PPP solutions is improved by 73.4 % from 27.4 to 7.3 mm with GPS-specific PCV corrections.

Figures 3 and 4 display positioning repeatability (STD) and accuracy (RMS) of GLONASS-only PPP solutions of the 218 stations, with the differences of STD and RMS values between the two solutions using the GLONASS- and GPS-specific PCVs. The stations of x-axis are arranged by station number (from Group 1 to 24, stations of each group are numbered in alphabetical order) in Table 1. From Figure 3, we can see that the differences of positioning repeatability by using GPS- and GLONASS-specific PCVs are very small. Concerning the RMS statistic, though the differences of horizontal values are also negligible as shown in Figure 4, the averaged RMS for the vertical component is improved by 10.7% from 8.4 to 7.5 mm by employing the GLONASS-specific rather than GPS-specific PCV corrections. Specifically, it is more significant for the stations equipped with LEIAR25.R3/NONE and LEIAR25.R3/LEIT antennas (Group 9 and 10).

From the above analysis, it is concluded that the effect of PCVs is non-ignorable in high-precision positioning. Though some systematic biases exist in up component for the GLONASS-only PPP by taking the GPS-specific PCVs, the daily repeatability turns out to be comparable with either GLONASS- or GPS-specific PCVs model. Thus, in the following demonstration, for the 33 stations denoted with green triangles in Figure 1, the GPS PCV corrections are applied in the GLONASS involved PPP and ZTD evaluation.

3.3. PERFORMANCE OF GLONASS IN PPP AND ZTD ESTIMATION

The overall performance of GLONASS in PPP is then studied with all the 251 stations by the comparison of GPS-, GLONASS-only, and GPS+GLONASS combined PPP in terms of positioning biases, repeatability, and accuracy. The stations of x-axis are again arranged by station numbers. The averaged biases of the stations with JAV_RINGANT_G3T/NONE (in red stars, see Figure 1) in east and north components for GLONASS-only PPP are –5.2 and –9.0 mm, respectively. They are abnormally larger than those of the other groups. From Figures 2 and 4, the impact of PCV corrections on horizontal position is small. Hence, we consider these horizontal biases may be caused by the inaccurate PCO corrections. Figure 5 shows no obvious antenna/radome-dependent biases in the horizontal and vertical components except the stations with JAV_RINGANT_G3T/NONE. As can be seen in Figures 6 and 7, better positioning repeatability and accuracy are found in north component than that in east component. One reason may be that the phase ambiguities are more correlated with the east component than the north component except in regions of high-latitude, the solutions of east component can be weakened through their correlation with phase ambiguities (Blewitt, 1989). The other reason may relate to the north-south ground tracks of GPS and GLONASS satellites in the earth-fixed reference frame (Melbourne, 1985).

Apart from the stations with JAV_RINGANT_G3T/NONE, the averaged RMS values of GLONASS-only PPP in east and north components are 3.8 and 2.6 mm, which are comparable to that of GPS-only PPP. GPS+GLONASS combined PPP get the smallest RMS values, 2.8, 2.2, and 5.6 mm in east, north, and up components, indicating that adding GLONASS observations can achieve better positioning performance than GPS-only PPP.

The impact of using or adding GLONASS observations on ZTD estimates is also discussed. With IGS final ZTD as reference (Byun and Bar-Sever, 2009), Figure 8 shows the biases of GPS-, GLONASS-only, and GPS+GLONASS PPP-derived ZTD. No latitude- or antenna/radome-dependent ZTD biases derived from GLONASS-only PPP can be observed. The biases range from -4.1 to 7.3 mm for GPS-only PPP-derived ZTD, from –6.0 to 8.0 mm for GLONASS-only, and from –3.5 to 7.2 mm for

GPS+GLONASS. Four stations have larger biases than the others, with CAS1 (66.2834°S, 110.5197°E), DAV1 (68.5773°S, 77.9726°E), and SYOG (69.0070°S, 39.5837°E) in Antarctica and MKEA (19.8014°N, 155.4563°W) on Hawaii island. Xu et al. (2015) indicated that, compared to elevation cutoff angle of 10°, the height accuracy can be improved by 25% for stations in Antarctic at elevation cutoff angle of 5° due to more low elevation angle observations. The ZTD and height parameters are more correlated. The elevation cutoff angle of 5° was selected in this study, while the IGS final ZTD products were processed at elevation cutoff angle of 7° (Byun and Bar-Sever, 2009). The larger ZTD biases on the three stations may be caused by the setting of elevation cutoff angle in the data processing. However, the reason for station MKEA is still unclear. The correlation between GPS-, GLONASS-only, GPS+GLONASS PPP-derived ZTD and IGS final ZTD is given in Figure 9. The correlation coefficient of 90.9 % (190 of 209) of the stations for GPS-only, 89.5 % (187 of 209) for GLONASS-only, and 91.9 % (192 of 209) for GPS+GLONASS is larger than 0.95. As indicated in Figure 10, the ZTD RMS is also showing latitude- and antenna/radome-independent. The percentage of the stations whose RMS values are smaller than 10 mm is about 90.9 % (190 of 209) for GPS-only, 85.7 % (179 of 209) for GLONASS-only, and 91.4 % (191 of 209) for GPS+GLONASS. The averaged ZTD accuracy is 7.8 mm for GPS-only, 8.1 mm for GLONASS-only, 7.7 mm for GPS+GLONASS, indicating that adding GLONASS observations can achieve slightly better performance in ZTD retrieval than that of GPS-only PPP.

4. CONCLUSIONS

In this study, we focused on position and ZTD estimates by adding GLONASS observations. First, we assessed PCVs effect on GLONASS positioning. By using GPS-specific PCVs, the averaged vertical RMS values of 33 stations, which did not have the GLONASS-specific PCVs, were reduced by 73.4 % from 27.4 to 7.3 mm. With GLONASS-specific PCVs, the averaged vertical RMS values of 218 stations, which both had GPS- and GLONASS-specific PCVs, were reduced by 10.7 % from 8.4 to 7.5 mm. By dividing the selected 251 stations into 30 groups by antenna/radome types, we further assessed the antenna/radome-dependent positioning biases for GLONASS-only PPP. There were no obvious antenna/radome-dependent biases except the stations with JAV_RINGANT_G3T/NONE in horizontal component especially in north component. The averaged biases of these stations in east and north components were –5.2 and –9.0 mm, respectively, which were abnormally larger than that of the other stations. Zheng et al. (2012) found there was a significant bias in the east component for station POTS with JAV_RINGANT_G3T/NONE. Unlike their results, we found that the stations with JAV_RINGANT_G3T/NONE all exhibited obvious systematic biases not only in east but also in north components. Apart from these stations, the averaged STD and RMS values in horizontal component for GPS- and GLONASS-only PPP were comparable, while GLONASS-only PPP obtained larger averaged vertical STD and RMS. The STD and RMS values of GPS+GLONASS combined PPP were the smallest, indicating that adding GLONASS observations could achieve better positioning performance than GPS-only. Also, better positioning repeatability and accuracy were found in north component than that in east component, which may be caused by the GNSS orbit configuration.

Meanwhile, the impact of using or adding GLONASS observations on ZTD estimates was also evaluated. The results showed that ZTD biases and accuracy of GLONASS-only are latitude- and antenna/radome-independent. The averaged ZTD accuracy was 7.8 mm for GPS-only, 8.1 mm for GLONASS-only, and 7.7 mm for GPS+GLONASS. No obvious biases between GPS- and GLONASS-only PPP-derived ZTD were observed, which were also confirmed by Lu et al. (2016) and Dousa and Vaclavovic (2016). Unlike positioning, we found that the ZTD accuracy improved by adding GLONASS observations is not obvious.

ACKNOWLEDGMENTS

Feng Zhou is financially supported by the China Scholarship Council (CSC) for his study at the German Research Centre for Geosciences GFZ. Many thanks go to the IGS for providing GNSS ground tracking data, precise orbit and clock products. This work is sponsored by National Natural Science Foundation of China (No. 61372086), Jiangxi Province key lab for digital land (No. DLLJ201701) and the Science and Technology Commission of Shanghai (No. 13511500300, No. 15511101602).

REFERENCES

Alcay, S., Inal, C., Yigit, C.O. and Yetkin, M.: 2012, Comparing GLONASS- only with GPS-only and hybride positioning in various length of baselines. Acta. Geod. Geophys. Hung., 47, 1, 1–12. DOI: 10.1556/AGeod.47.2012.1.1

Anquela, A.B., Martín, A., Berné, J.L. and Padin, J.: 2013, GPS and GLONASS static and kinematic PPP results. J. Surv. Eng., 139, 1, 47–58. DOI: 10.1061/(ASCE)SU.1943-5428.0000091

Baire, Q., Pottiaux, E., Bruyninx, C., Defraigne. P, Aerts, W., Legrand, J., Bergeot. N. and Chevalier, J.M.: 2014, Influence of different GPS receiver antenna calibration models on geodetic positioning. GPS Solut., 18, 4, 529–539. DOI: 10.1007/s10291-013-0349-1

Blewitt, G.: 1989, Carrier phase ambiguity resolution for the global positioning system applied to geodetic baselines up to 2000 km. J. Geophys. Res., 94, B8, 10187–10203. DOI: 10.1029/JB094iB08p10187

Bock, Y. and Melgar, D.: 2016, Physical applications of GPS geodesy: A review. Rep. Prog. Phys., 79, 106801, 119 pp.
DOI: 10.1088/0034-4885/79/10/106801

Boehm, J., Niell, A., Tregoning, P. and Schuh, H.: 2006, Global mapping function (GMF): A new empirical mapping function based on numerical weather model data. Geophys. Res. Lett., 33, L07304.
DOI: 10.1029/2005GL025546

Bruyninx, C.: 2007, Comparing GPS-only with GPS + GLONASS positioning in a regional permanent GNSS network. GPS Solut., 11, 2, 97–106.
DOI: 10.1007/s10291-006-0041-9

Byun, S.H., and Bar-Sever, Y.E.: 2009, A new type of troposphere zenith path delay product of the international GNSS Service. J. Geod., 83, 3, 367–373.
DOI:10.1007/s00190-008-0288-8

Cai, C. and Gao, Y.: 2007, Precise point positioning using combined GPS and GLONASS observations. J. Glob. Positioning. Syst., 6, 1, 13–22.

Cai, C. and Gao., Y.: 2013, GLONASS-based precise point positioning and performance analysis. Adv. Space Res., 51, 3, 514–524. DOI: 10.1016/j.asr.2012.08.004

Chen, G. and Herring, T.A.: 1997, Effects of atmospheric azimuthal asymmetry on the analysis of space geodetic data. J. Geophys. Res., 102, B9, 20489–20502. DOI: 10.1029/97JB01739

Defraigne, P. and Baire, Q.: 2011, Combining GPS and GLONASS for time and frequency transfer. Adv. Space Res., 47, 2, 265–275.
DOI: 10.1016/j.asr.2010.07.003

Dilssner, F., Springer, T., Flohrer, C. and Dow, J.: 2009, Estimation of phase center corrections for GLONASS-M satellites antennas. J. Geod., 84, 8, 467–480.
DOI: 10.1007/s00190-010-0381-7

Dousa, J.: 2010, Precise near real-time GNSS analyses at geodetic observatory Pecny-precise orbit determination and water vapour monitoring. Acta Geodyn. Geomater., 7, 1(157), 7–17.

Dousa, J. and Vaclavovic, P.: 2016, Evaluation of ground-based GNSS tropospheric products at Geodetic Observatory Pecny. In: IAG 150 Years, Rizos, Ch. and Willis, P. (eds), IAG Symposia Series, 143, 759–766. DOI: 10.1007/1345_2015_157

Fritsche, M., Sosnica, K., Rodríguez-Solano, C.J., Steigenberger, P., Dietrich, R., Dach, R., Wang, K., Hugentobler, U. and Rothacher, M.: 2014, Homogeneous reprocessing of GPS, GLONASS and SLR observations. J. Geod., 88, 7, 625–642.
DOI: 10.1007/s00190-014-0710-3

Gu, S., Shi, C., Lou, Y. and Liu, J.: 2015, Ionospheric effects in uncalibrated phase delay estimation and ambiguity-fixed PPP based on raw observable model. J. Geod., 89, 5, 447–457.
DOI: 10.1007/s00190-015-0789-1

He, P., Wang, Q., Ding, K., Li, J. and Zou, R.: 2016, Coseismic and postseismic slip ruptures for 2015 Mw 6.4 Pishan earthquake constrained by static GPS solutions. Geodesy and Geodynamics, 7, 5, 323–328.
DOI: 10.1016/j.geog.2016.07.004

Li, X., Dick. G., Ge, M., Heise, S., Wickert. J. and Bender, M.: 2014, Real-time GPS sensing of atmospheric water vapor: precise point positioning with orbit, clock and phase delay corrections. Geophys. Res. Lett., 41, 10, 3615–3621.
DOI: 10.1002/2013GL058721

Liu, J. and Ge, M: 2003, PANDA software and its preliminary result of positioning and orbit determination. Wuhan Univ. J. Nat. Sci., 8, 2B, 603–609. DOI: 10.1007/BF02899825

Liu, Z., Li, Y., Guo, J. and Li, F.: 2016, Influence of higher-order ionospheric delay correction on GPS precise orbit determination and precise positioning. Geodesy and Geodynamics, 7, 5, 369–376.
DOI: 10.1016/j.geog.2016.06.005

Lou, Y., Zheng, F., Gu, S., Wang, C., Guo, H. and Feng, Y.: 2016, Multi-GNSS precise point positioning with raw single-frequency and dual-frequency measurement models. GPS Solut., 20, 4, 849–862.
DOI: 10.1007/s10291-015-0495-8

Lu, C., Li, X., Ge, M., Heinkelmann, R., Nilsson, T, Soja, B. and Schuh, H.: 2016, Estimation and evaluation of real-time precipitable water vapor from GLONASS and GPS. GPS Solut., 20, 4, 703–713.
DOI: 10.1007/s10291-015-0479-8

Melbourne, W.G.: 1985, The case for ranging in GPS based geodetic systems. In Proceedings of the First Symposium on Precise Positioning with the Global Positioning System, Positioning with GPS-1985, U.S. Department of Commerce, Rockville, Md., 373–386.

Ning, T., Elgered. G., Willen, U. and Johansson, J.M.: 2013, Evaluation of the atmospheric water vapor content in a regional climate model using ground-based GPS measurements. J. Geophys. Res., 118, 1–11.
DOI: 10.1029/2012JD018053

Saastamoinen, J.: 1973, Contributions to the theory of atmospheric refraction Part II. Refraction corrections in satellite geodesy. J. Bull. Geodesique, 107, 1,13–34. DOI: 10.1007/BF02522083

Schmid, R., Dach, R., Collilieux, X., Jäggi, A., Schmitz, M. and Dilssner, F.: 2016, Absolute IGS antenna phase center model igs08.atx: status and potential improvements. J. Geod., 90, 4, 343–364.
DOI: 10.1007/s00190-015-0876-3

Xu, Y., Jiang, N., Xu, G., Yang, Y. and Schuh, H.: 2015, Influence of meteorological data and horizontal gradient of tropospheric model on precise point positioning. Adv. Space Res., 56, 11, 2374–2383.
DOI: 10.1016/j.asr.2015.09.027

Zheng, Y., Nie, G., Fang, R., Yin, Q., Yi, W. and Liu, J.: 2012, Investigation of GLONASS performance in differential positioning. Earth Sci. Inform., 5, 3, 189–199. DOI: 10.1007/s12145-012-0108-9

Zinoviev, A.E.: 2005, Using GLONASS in combined GNSS receivers: Current status. Proc. ION GNSS-2005, Long Beach, CA, 1046–1057.

Zumberge, J.F., Heflin, M.B., Jefferson, D.C., Watkins, M.M. and Webb, F.H.: 1997, Precise point positioning for the efficient and robust analysis of GPS data from large networks. J. Geophys. Res., 102, B3, 5005–5018. DOI: 10.1029/96JB03860

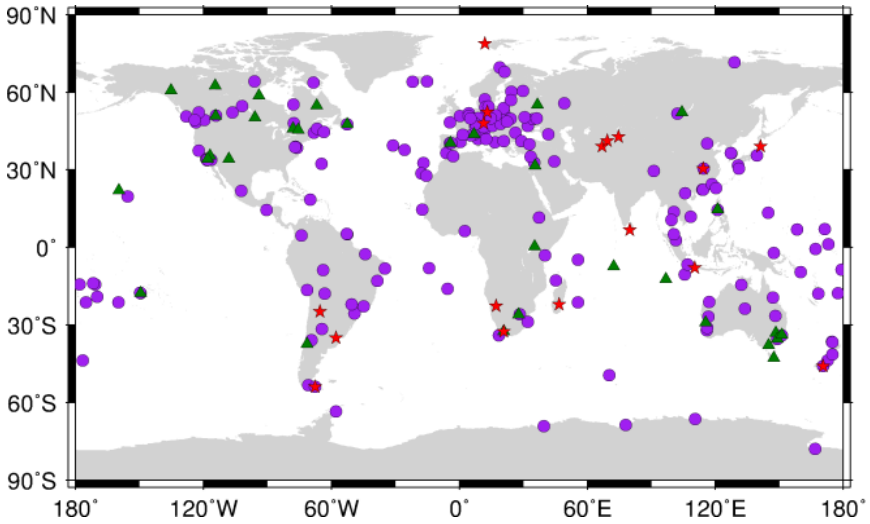

Fig. 1 Geographical distribution of 251 IGS tracking stations used in the experiment. The red stars indicate the stations with antenna/radome type of JAV_RINGANT_G3T/NONE (see Group 21 in Table 1); The purple solid dots and red stars represent the 218 stations with GLONASS-specific antenna/radome calibrations (see Group 1-24 in Table 1), and green triangles denote the 33 stations without such calibrations (see Group 25-30 in Table 1).

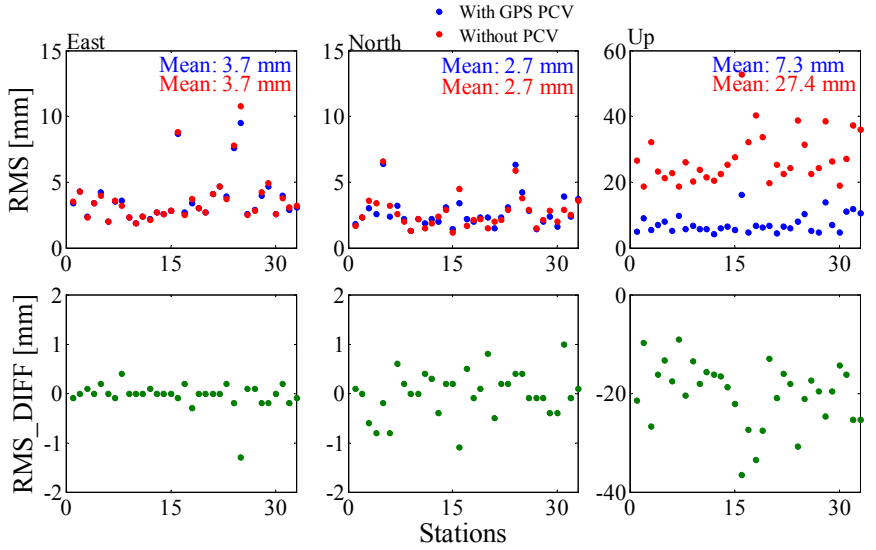

Fig. 2 The positioning accuracy of GLONASS-only PPP solutions of the 33 stations in east, north, and up components; the differences (DIFF) of RMS between with and without GPS PCVs are also displayed.

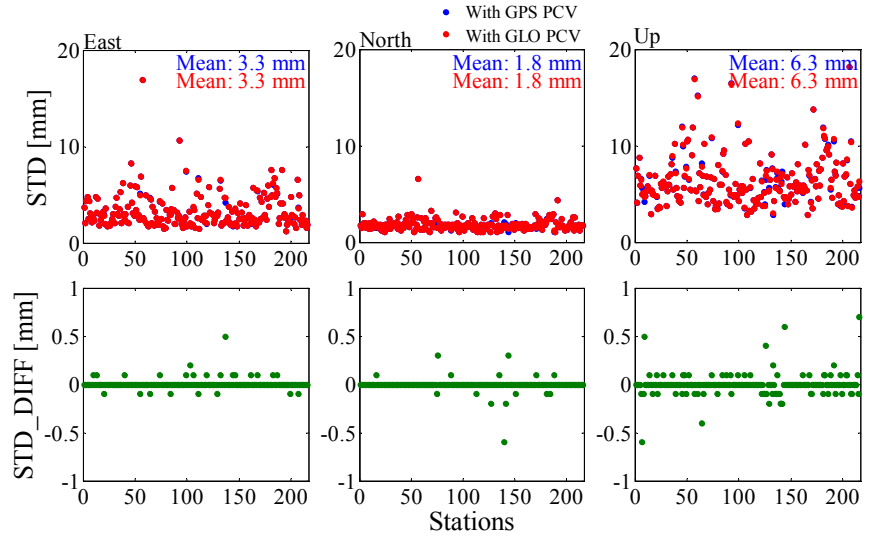

Fig. 3 The positioning repeatability of GLONASS-only PPP solutions of the 218 stations in east, north, and up components; the differences (DIFF) of STD between "With GLO PCV" and "With GPS PCV" are also displayed.

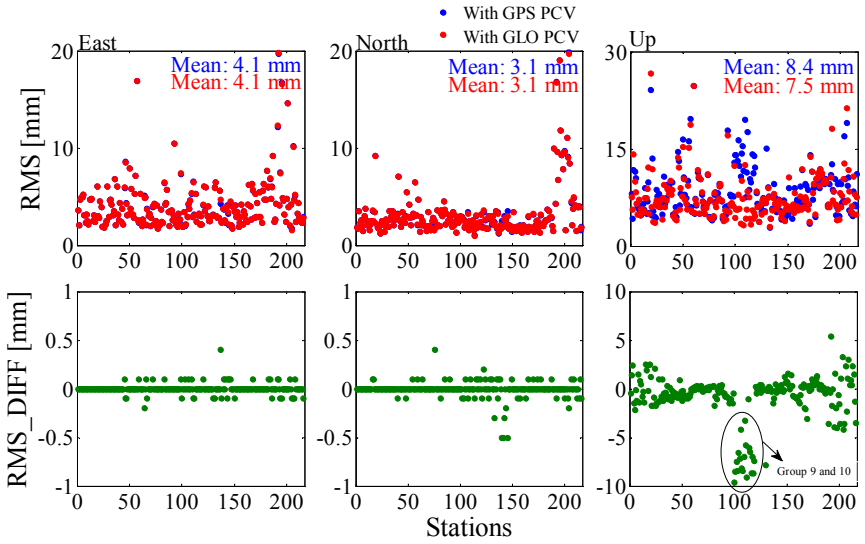

Fig. 4 The positioning accuracy of GLONASS-only PPP solutions of the 218 stations in east, north, and up components; the differences (DIFF) of RMS between "With GLO PCV" and "With GPS PCV" are also displayed.

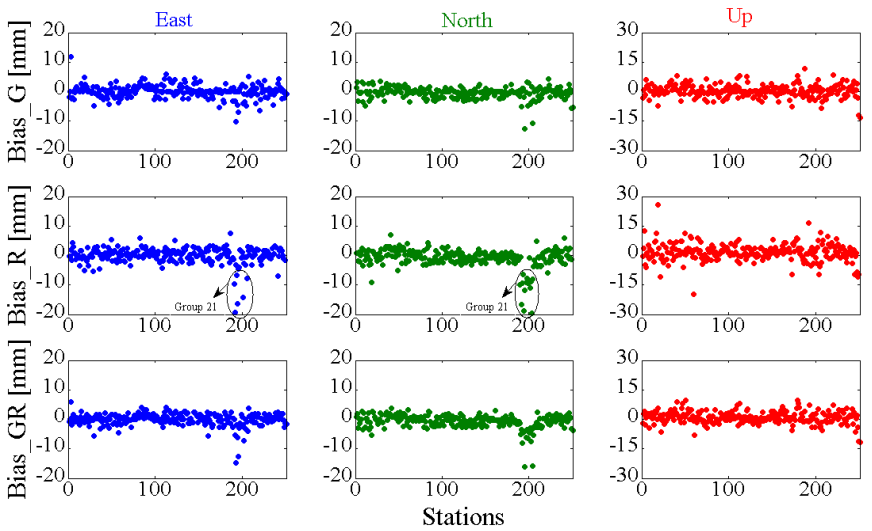

Fig. 5 The positioning biases of GPS-only (G), GLONASS-only (R), and GPS+GLONASS (GR) PPP solutions of 251 stations in east, north, and up components.

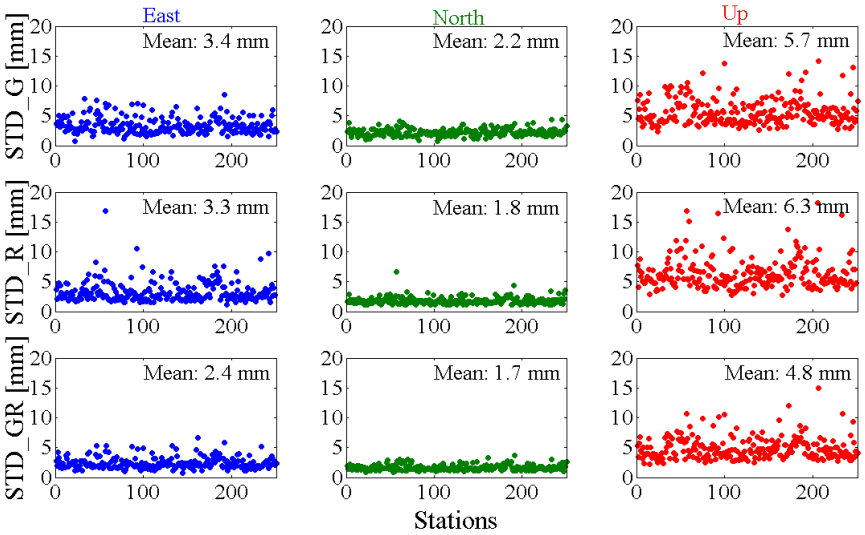

Fig. 6 The positioning repeatability of GPS-only (G), GLONASS-only (R), and GPS+GLONASS (GR) PPP solutions of 251 stations in east, north, and up components.

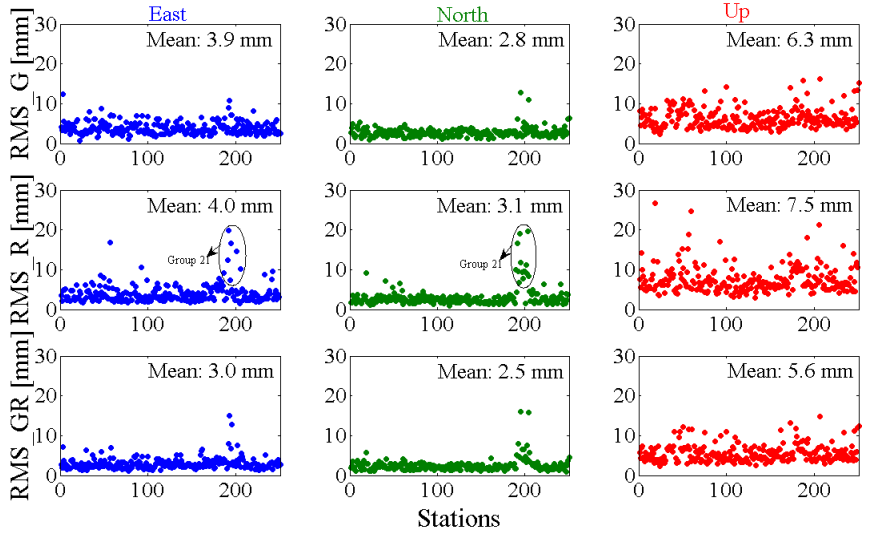

Fig. 7 The positioning accuracy of GPS-only (G), GLONASS-only (R), and GPS+GLONASS (GR) PPP solutions of 251 stations in east, north, and up components.

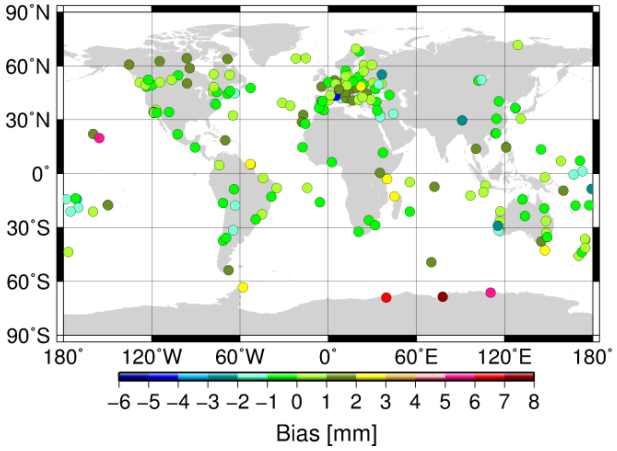

(a)

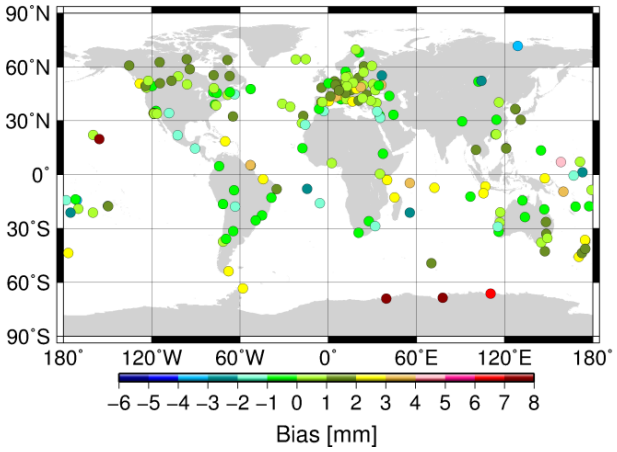

(b)

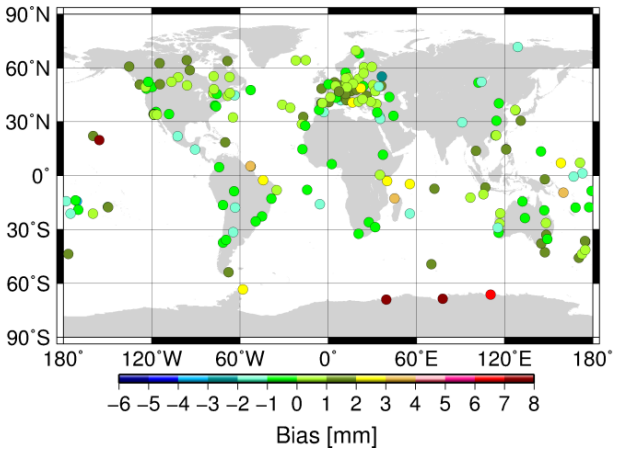

(c)

Fig. 8 The biases of GPS- (a), GLONASS-only (b) and GPS+GLONASS (c) PPP-derived ZTD with respect to IGS final ZTD of 209 stations.

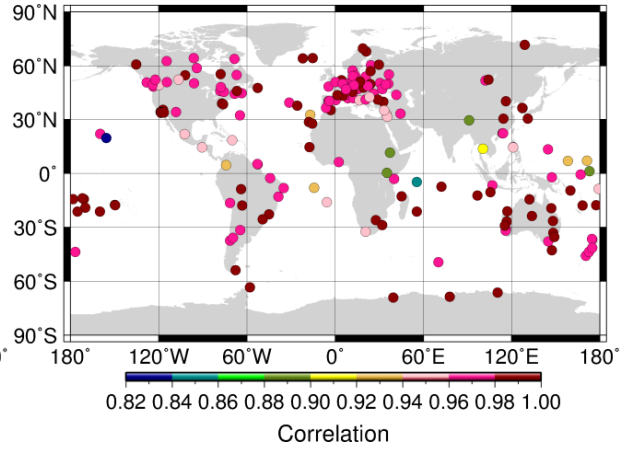

(a)

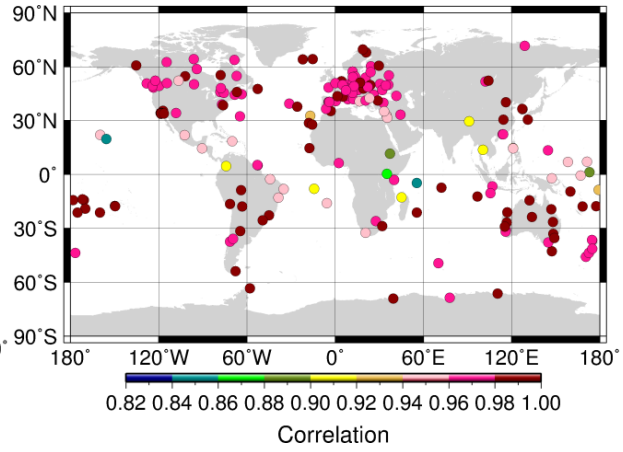

(b)

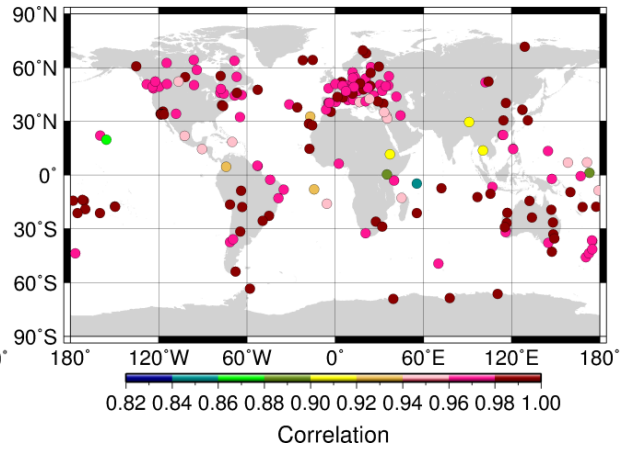

(c)

Fig. 9 The correlation between GPS- (a), GLONASS-only (b), GPS+GLONASS (c) PPP-derived ZTD and IGS final ZTD of 209 stations.

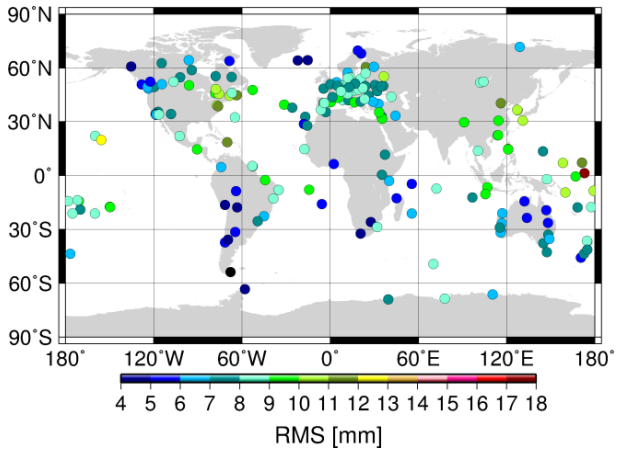

(a)

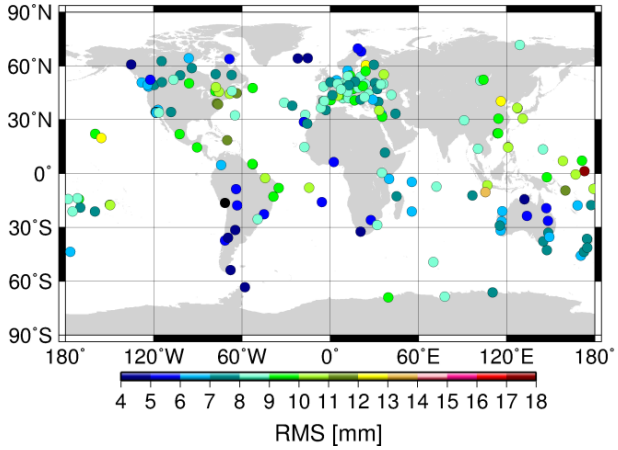

(b)

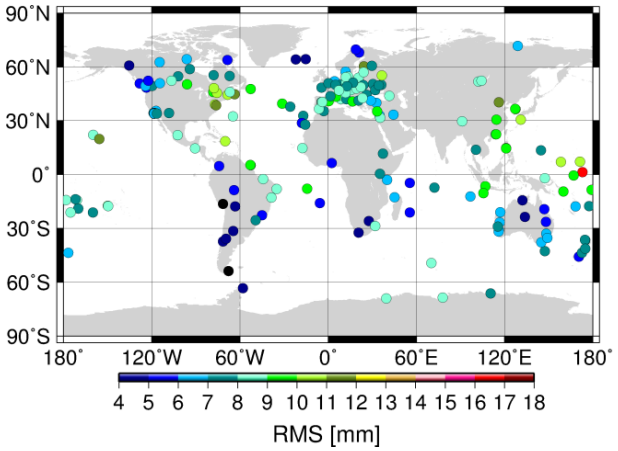

(c)

Fig. 10 The RMS of GPS- (a), GLONASS-only (b) and GPS+GLONASS (c) PPP-derived ZTD with respect to IGS final ZTD of 209 stations.